https://doi.org/10.5194/bg-2020-58
Preprint. Discussion started: 25 March 2020

Biogeosciences Discussions
Open Access
EGU

The Role of Sediment-induced Light Attenuation on Primary Production during Hurricane Gustav (2008)

Zhengchen Zang[1], Z. George Xue[1,2,3 *], Kehui Xu [1,3], Samuel J. Bentley [3,4], Qin Chen[5], Eurico J. D'Sa[1,3], Le Zhang[1], Yanda Ou[1]

[1] Department of Oceanography and Coastal Sciences, Louisiana State University, Baton Rouge, LA 70803, USA (now at Woods Hole Oceanographic Institution, Woods Hole, MA, 02543)

[2] Center for Computation and Technology, Louisiana State University, Baton Rouge, LA 70803, USA

[3] Coastal Studies Institute, Louisiana State University, Baton Rouge, LA 70803, USA

[4] Department of Geology and Geophysics, Louisiana State University, Baton Rouge, LA 70803, USA

[5] Department of Civil and Environmental Engineering, Northeastern University, Boston, MA 02115, USA

Corresponding author: Z. George Xue (zxue@lsu.edu)

Key Words:

Gulf of Mexico; Sediment-induced light attenuation; hurricane; offshore bloom.

https://doi.org/10.5194/bg-2020-58
Preprint. Discussion started: 25 March 2020

Biogeosciences Discussions

Abstract

We introduced a sediment-induced light attenuation algorithm into the biogeochemical model of the Coupled Ocean-Atmosphere-Wave-Sediment Transport (COAWST) modeling system. A fully coupled ocean-atmospheric-sediment-biogeochemical simulation was carried out to assess the impact of sediment-induced light attenuation on primary production in the northern Gulf of Mexico during Hurricane Gustav in 2008. The new model showed a better agreement with satellite data on both the magnitude of nearshore chlorophyll concentration and the distribution of offshore bloom. When Gustav approached, resuspended sediments shifted the inner shelf ecosystem from a nutrient-limited one to light-limited. One week after Gustav's landfall, accumulated nutrient and favorable optical environment induced a post-hurricane algal bloom in the top 20 m of water column, while the productivity in the lower layer was still light-limited due to unsettled sediment. Corresponding with the elevated offshore NO_3 flux (38.71 mmol N/m/s) and decreased chlorophyll flux (43.10 mg/m/s), the post-hurricane bloom in the outer shelf was resulted from the cross-shelf nutrient supply instead of the lateral dispersed chlorophyll. Sensitivity tests indicated that sediment light attenuation efficiency affected primary production when sediment concentration was moderately high. The influence of terrestrial nutrient discharge on primary production was dominant after three days of hurricane landfall and kept increasing until the end of model simulation. Model uncertainties were also discussed.

1 Introduction

Light is the primary agent for photosynthesis and plays a vital role in marine ecosystems. The vertical structure of light availability in an aquatic environment is mainly modulated by the shading effects of chlorophyll, colored dissolved organic matter (CDOM), detritus, and sediment (Cloern, 1987; Devlin et al., 2008; Schaeffer et al., 2011; Ganju et al., 2014; McSweeney et al., 2017). The optical environments in river-dominated shelves are more complex due to the high spatiotemporal variations of light absorbers caused by the interaction between riverine inputs and regional hydrodynamics (Bierman et al., 1994; Lin et al., 2009; Zhu et al., 2009). As the largest river in North America, the Mississippi-Atchafalaya River system delivers 380 km^3 of freshwater and 115 Mt of sediments each year into the northern Gulf of Mexico (nGoM; Meade and Moody, 2010; Allison et al., 2012). Over the Louisiana-Texas shelf in the nGoM, suspended sediment concentration (SSC) in the water column exhibits strong seasonality: SSC in winter and spring seasons is high due to strong sediment resuspension and large fluvial sediment discharge; while in summer and fall it is largely reduced owing to the relatively low river inputs and weak resuspension (Zang et al., 2019). Episodic hurricane events in summer and fall can disturb vertical stratification and resuspend large amount of sediment (D'Sa et al., 2011; Xu et al., 2016; Zang et al., 2018). Enhanced resuspension during a hurricane might greatly change the shelf ecosystem via modifying light availability, yet the related studies are limited due to the challenge of *in-situ* data collection under extreme weather conditions. In addition to light attenuation, another potential impact from resuspended sediment is enhanced organic matter remineralization in the bottom boundary layer (Wilson et al., 2013; Hurst et al., 2019), yet so far available field studies are still very limited.

As an alternative tool to fill the spatial and temporal gaps in *in-situ* datasets, coupled physical-biogeochemical models have been widely applied to the Gulf of Mexico (e.g. Fennel et al., 2008; Laurent et al., 2012; Xue et al., 2013; Yu et al., 2015; Gomez et al., 2018). Although most of these studies considered sediment-induced light attenuation when estimating primary

https://doi.org/10.5194/bg-2020-58
Preprint. Discussion started: 25 March 2020

production, its influence remained unchanged over the entire research domain and did not vary with sediment dynamics. Such an oversimplified treatment of sediment-induced light attenuation could substantially impact models' robustness in river-dominated shelves that encompass a wide range of SSC. Justić and Wang (2014) tentatively employed a new scheme by connecting sediment-induced light attenuation with river discharge (salinity) and hydrodynamics (bottom shear stress) in the nGoM. However, the horizontal distribution of SSC in a realistic environment is not necessarily correlated with that of the freshwater plume, and the contribution of resuspension to SSC in different vertical layers might vary significantly (Xu et al., 2011).

Gustav was the first major hurricane that made a landfall in Louisiana after Katrina (2005). It passed through the center of GoM and landed near Cocodrie, Louisiana on September 1st of 2008 as a Category 2 hurricane (Forbes et al., 2010). Sediment resuspension and transport were strong during the passage of Gustav, and thick post-hurricane deposition (up to 40 cm) was simulated on the inner shelf (Zang et al., 2018) and in the bays (Liu et al., 2018). Korobkin et al. (2009) identified a post-Gustav algal bloom around the Mississippi Delta using satellite images. High respiration and stratification after the landfall of Gustav was reported to be connected with hypoxia development on the shelf (McCarthy et al., 2013). In this study, we built a biogeochemical model with sediment-induced light attenuation on the hydro- and sediment dynamics of the three-way coupled (atmospheric-wave-ocean) Gustav model (Zang et al., 2018). It is worth of note that sediment dynamics can also impact nutrient dynamics via changing the intensity of remineralization near the bottom (Moriarty et al., 2018). However, in this study we only investigated the influence of suspended sediment on optical environment and primary production. The impact from elevated remineralization of resuspended particular organic matter was not considered as detailed processes in water column and sediment bed because their relevant parameterizations during extreme weather events are still largely unknown. Our objectives are to: 1) evaluate the impact of sediment-induced light attenuation on the spatiotemporal variation of nutrient-phytoplankton dynamics during a hurricane event; 2) explore the driving mechanism of the post-hurricane bloom on the shelf; and 3) investigate the response of primary production to sediment optical characteristics and fluvial nutrient input.

2 Model Description

2.1 Physical, sediment and biogeochemical models

Our model covered the entire GoM (Fig. 1a) and was built on the coupled ocean-atmosphere-wave-and-sediment transport (COAWST) modeling system (Warner et al., 2008, 2010). COAWST is an open source model platform that consists of three numerical models: the Weather Research and Forecasting model (WRF; Skamarock et al., 2005), the Regional Ocean Modeling System (ROMS; Shchepetkin and McWilliams, 2005; Haidvogel et al., 2008), and the Simulating Waves Nearshore model (SWAN; Booij et al., 1999). The Community Sediment Transport Modeling System (CSTMS) is included in ROMS to simulate sediment dispersal, stratigraphy, and geomorphology. Model Coupling Toolkit (MCT; Jacob et al., 2005) enables the interaction among the three models. Details of model setup and validation of the three-way coupled hydrodynamic-sediment transport model (WRF-ROMS-SWAN-CSTMS) was described in Zang et al. (2018). The biogeochemical model in this study was largely built on the North Pacific Ecosystem Model for Understanding Regional Oceanography (NEMURO; Kishi et al., 2007), which incorporated both nitrogen and silicon flows. Eleven state variables were included in the model: nitrate, ammonium, two types of phytoplankton (small and large), three types of zooplankton (microzooplankton, mesozooplankton and predatory zooplankton), particulate and

https://doi.org/10.5194/bg-2020-58
Preprint. Discussion started: 25 March 2020

dissolved nitrogen, particulate silica, and silicic acid concentration. We incorporated two types of chlorophyll corresponding to the large and small phytoplankton tracers, respectively. The estimation of chlorophyll concentration was based on Fennel et al. (2006). To get an ideal parameterization set and a stable initial condition for the biogeochemical variables, we first conducted a 20-yr (1993-2012) coupled physical-biogeochemical simulation using the same model domain with the WRF and SWAN models disabled to achieve a feasible computation load (step 1 in Fig. 2). Instead, the atmospheric forcing was provided by the 6-hourly, 38 km horizontal resolution Climate Forecast System Reanalysis (CFSR; Saha et al., 2010, 2011; http://cfs.ncep.noaa.gov). The physical setup of the 20-yr simulation was the same as Zang et al. (2019). The biogeochemical parameterizations (Table. S1) were largely adapted after a recent GoM biogeochemical modeling study by Gomez et al. (2018). Since this study focused on the response of biogeochemical process to hurricane event, details of the 20-yr simulation setup and model-observation comparison were provided in the supplementary material. Once validated, the biogeochemical variables were extracted from the 20-yr model on August 30th, 2008 as the initial condition for the Gustav simulation (step 2 in Fig. 2).

The light available for photosynthesis (I) is estimated using the following equation:

$$I = I_0 exp\{-Z[\alpha_w + \alpha_{chl}(PSn + PLn) + \alpha_{sed} SSC]\},$$

where I_0 is light intensity at the surface layer, and Z is water depth. α_w and α_{chl} are light extinction coefficient of sea water and self-shading coefficient, respectively. PSn and PLn represent concentrations of small phytoplankton and large phytoplankton. Compared with original biogeochemical model, we added a new sediment-induced light attenuation term ($\alpha_{sed} SSC$) to this equation. α_{sed} is light extinction coefficient due to suspended sediment, and SSC is total suspended sediment concentration in the certain layer. We performed a benchmark run (α_{sed} = 0.059; McSweeney et al., 2017) to represent the scenarios with sediment-induced light attenuation. The simulation period was from August 30th to September 10th, 2008.

2.2 Sensitivity tests

High turbidity in the Mississippi River estuary due to fluvial sediment discharge and resuspension suggested the vital role of sediment in underwater optical environment. To quantitatively evaluate the importance of suspended sediment in light attenuation, we conducted a sensitivity test (test 1) without sediment-induced light attenuation term ($\alpha_{sed} = 0$). Since the physical properties of sediment particle (e.g., size, shape, roughness, and color) determined its light attenuation efficiency (Baker and Lavelle, 1984; Storlazzi et al., 2015), a wide range of α_{sed} has been applied in previous studies (e.g., Pennock, 1985; Arndt et al., 2007; McSweeney et al., 2017). Here we selected $\alpha_{sed} = 0.075$ (test 2; Pennock, 1985) and $\alpha_{sed} = 0.025$ (test 3; Van Duin et al., 2001) to represent high/low attenuation efficiency and examined the sensitivity of primary production to sediment-induced light attenuation.

3 Model Validation

Direct measurements of ocean conditions during the passage of a hurricane remained a major challenge. In Zang et al. (2018) we validated the physical model's performance against the air pressure, sea level, and wave heights recorded at available buoy stations. The sediment model's performance was evaluated against satellite images. In this study, we used the five-day composites of SeaWiFS satellite images before (Aug 25th–29th) and after (September 5th–9th) Gustav's landing

https://doi.org/10.5194/bg-2020-58
Preprint. Discussion started: 25 March 2020

to calibrate our biogeochemical model. The satellite images showed higher chlorophyll concentration around the bird-foot delta and on the Atchafalaya shelf in the post-hurricane composite than the pre-hurricane one (Figs. 3a and 3b). Another major difference between the two composites was identified in the waters between the 50 and 200 m isobaths off the Atchafalaya Bay: chlorophyll concentration increased from 1 to 4 mg/m^3 after Gustav, indicating a possible post-hurricane algal bloom on the outer shelf. The intensity of offshore bloom was better reproduced (~ 4 mg/m^3) with the new sediment-induced light attenuation algorithm (benchmark run, see difference between Figs. 3c and 3d). To quantitatively evaluate model's performance, we calculated the root mean square error (RMSE) and correlation coefficient (R) between model-simulated and satellite-based chlorophyll concentrations over the inner shelf (water depth < 50 m; Fig. 4). The reduced RMSE in the benchmark run in comparison to sensitivity test (2.33 to 1.91) suggested model performance was improved by including sediment-induced light attenuation. The correlation coefficients were slightly different (0.82 and 0.81), indicating the spatial distributions of chlorophyll of the two experiments were comparable (Fig. 4). Nevertheless, model's performance was significantly improved in high productivity waters where chlorophyll concentration is > 1 mg/m^3: R increased from 0.55 to 0.61, and RMSE decreases from 5.93 to 3.97 (Fig. 4). The improvement of model results confirmed the significance of sediment-induced light attenuation in biogeochemical cycling during hurricane Gustav, particularly in coastal regions where chlorophyll concentration was high.

4 Results and Discussion

4.1 Temporal variability of biogeochemical variables

To examine the temporal variation of biogeochemical variables during the passage of Gustav, we plotted the time series of spatially averaged net primary production (NPP), surface chlorophyll concentration, NO_3 concentration, SSC, short wave radiation, and sea surface temperature (SST) over the nGoM inner shelf (< 50 m water depth; Fig. 5). NPP exhibited strong diel variation and the peaks were strongly correlated with short wave radiation maximum (Figs. 5a and 5e). Such diel cycle could also be found in chlorophyll concentration, but with a 3 to 4-hour delay (Fig. 5c). Before the approach of Gustav, daily-averaged NPP was around 1 g C/m^2/day, and the differences of NPP and chlorophyll concentration between the benchmark run and test 1 were negligible (Fig. 5a).

When Gustav landed in coastal Louisiana at 16:00:00 UTC on September 1st, surface SSC went up to 3.8 kg/m^3 because of strong seabed erosion and resuspension (Fig. 5d). Daily-averaged NPP reduced to 0.7 g C/m^2/day in test 1. Once sediment-induced light attenuation was included, daily-averaged NPP further declined to 0.2 g C/m^2/day, suggesting that light availability severely limited short-term productivity on the inner shelf. Chlorophyll concentrations in the benchmark run and test 1 were reduced by 40% when hurricane approached. Hurricane-related surface cooling, together with decreased light (Figs. 5e and 5f), contributed to the reductions of chlorophyll and NPP.

Daily-averaged NPP difference between the two experiments maximized on September 2nd due to light limitation modulated by resuspended sediments (Figs. 5a and 5d). On September 3rd, daily-averaged NPP of test 1 recovered to 0.9 g C/m^2/day and was steady through the end of our simulation (Fig. 5a). For the benchmark run, however, the recovery of NPP was much slower: daily-averaged NPP was lower than that of test 1 until September 7th, when most suspended sediment settled back onto the seabed. NO_3 concentration went up gradually in the benchmark run from September 2nd to September 7th because nutrient consumption was constrained by the

https://doi.org/10.5194/bg-2020-58
Preprint. Discussion started: 25 March 2020

declined photosynthesis (Fig. 5c). Accumulated NO_3, together with the preferable optical environment due to low SSC, resulted in higher NPP and algal bloom after September 7th (Figs. 5a and 5b).

4.2 Vertical structure of biogeochemical variables

We extracted concentrations of chlorophyll and sediment along the transect D in Rabalais et al. (2001; location see Fig. 1b) at three time points (August 31st, September 2nd, and September 10th) to represent pre-, during-, and post-hurricane stages, respectively (Fig. 6). Before the approach of Gustav, chlorophyll concentration decreased seaward from 5 to 0.3 mg/m^3, and sediment-induced light attenuation did not alter the vertical structure of chlorophyll owing to low SSC in the water column (Figs. 6a–c). On September 2nd, strong resuspension elevated the SSC to more than 1 kg/m^3 over the entire water column (Fig. 6f). Chlorophyll concentration over the top 40 m in the benchmark run was ~ 4 mg/m^3 lower than that in test 1 due to sediment-induced light attenuation. The most dominant difference between the two simulations located nearshore where the water depth was < 20 m (Figs. 6d and 6e).

In test 1, chlorophyll concentration during the post-hurricane stage was lower than that of the pre-hurricane stage (Figs. 6a and 6g), which contradicted with the condition captured by satellite images (Figs. 3a and 3b). The benchmark run, however, successfully reproduced the magnitude and seaward extension of the post-hurricane bloom (Fig. 6h). High chlorophyll concentration (> 1 mg/m^3) was simulated in the top 20 m of the water column where sediment concentration was low after the passage of Gustav (Figs. 6g and 6h). As water depth exceeded 20 m, chlorophyll concentration dropped drastically to less than 0.1 mg/m^3. The synchronized high turbidity (Fig. 6i) and low chlorophyll concentration implied that, nine days after Gustav's landfall, the primary production in deep water could still be constrained by limited light availability. A similar vertical structure (high SSC and low chlorophyll at the bottom) was also simulated in the Delaware estuary, where near bottom productivity was constrained by the estuarine turbidity maximum (McSweeney et al., 2017). Such a well stratified water column with high/low productivity at the surface/bottom was in favor of bottom oxygen depletion: elevated surface phytoplankton growth after hurricane provided more particulate organic matter (POM), which could sink gradually and be decomposed in the bottom water with high oxygen consumption (Wiseman et al., 1997). Meanwhile, the post-hurricane stratification recovery in summer and fall seasons prevented oxygen ventilation to the bottom. Another major process that might further lower the oxygen level was the high respiration rate caused by resuspended POM (Bianucci et al., 2018). McCarthy et al. (2013) reported a post-Gustav respiration peak associated with organic matter resuspension in the bottom boundary layer. A recent numerical model study also supported substantial increase of near-bottom oxygen consumption due to resuspended POM remineralization during moderate resuspension events (Moriarty et al., 2018). These existing studies and the new finding of this study suggested particulate matter (both organic and inorganic) dynamics might substantially contribute to bottom oxygen depletion and hypoxia development.

4.3 The post-hurricane offshore bloom

Post-hurricane blooms have been widely observed in the mid- and low-latitude oceans (Davis and Yan, 2004; Miller et al., 2006; Pan et al., 2017). A bloom in the open ocean was usually isolated and patchy, and its formation was mainly related to nutrients and chlorophyll vertical mixing (Walker et al., 2005; Pan et al., 2017). The mechanism of the offshore bloom formation on the outer shelf, however, was more complex due to additional impacts from the inner shelf water.

https://doi.org/10.5194/bg-2020-58
Preprint. Discussion started: 25 March 2020

Strong cross-shore transport after hurricane Gustav has been reported by previous studies (Korobkin et al., 2009; Zang et al., 2018). The seaward dispersal of coastal waters with higher nutrient and chlorophyll concentrations might potentially result in the outer shelf bloom, while their respective contributions were still unclear. To quantify the cross-shore exported nutrient and chlorophyll, we estimated depth integrated offshore (seaward) NO_3 and chlorophyll flux along the 50 m isobath transect (location see Fig. 1b; Table. 1). Compared with test 1 (NO_3: 7.35 mmol N/m/s; Chlorophyll: 66.88 mg/m/s), the benchmark run simulated a higher NO_3 flux (38.71 mmol N/m/s) and a lower chlorophyll flux (43.10 mg/m/s). The differences in NO_3 and chlorophyll fluxes between the two simulations could be explained by nutrient accumulation and NPP reduction on the inner shelf when sediment-induced light attenuation was dominant (Figs. 5a and 5c). Given the better offshore bloom intensity reproduced by the benchmark run (Figs. 3c and 3d), we concluded that the cross-shore export of previously accumulated nutrient during low light availability significantly contributed to the post-hurricane offshore bloom.

4.4 Sensitivity to sediment light extinction coefficient (α_{sed})

Sediment light attenuation efficiency was determined by many physical properties of sediment particle (e.g., size, shape, roughness, and color), which resulted in the great challenge to reasonably parameterize α_{sed} over the entire nGoM (Baker and Lavelle, 1984; Storlazzi et al., 2015). To examine the sensitivity of primary production to sediment light attenuation efficiency, the results of sensitivity tests with different α_{sed} (tests 2 and 3) were compared with the benchmark run.

The difference of primary production between benchmark run and sensitivity tests 2 and 3 was limited before the landfall of hurricane Gustav (Fig. 7a). The insensitivity of sediment-induced light attenuation under normal condition suggested that the nGoM ecosystem was mainly limited by nutrient rather than light (Fennel et al., 2011). After 2 days of hurricane landfall (Sept 1st – 3rd), high SSC due to strong sediment resuspension suppressed photosynthesis in the entire water column (Fig. 7). The contribution of high SSC overwhelmed that of α_{sed} to the variation of sediment-induced light attenuation term ($\alpha_{sed}SSC$). Therefore, the primary production was still insensitive to α_{sed} from Sept 1st to Sept 3rd although the nGoM ecosystem was limited by light availability. After Sept 3rd, the primary production and NO_3 concentration of test 3 with lower α_{sed} exceeded those of benchmark run and test 2 until Sept 7th (Fig. 7). The sensitivity of primary production to α_{sed} during this period was caused by the decreased contribution of SSC to sediment-induced light attenuation associated with sediment settling (Fig. 5d). In the last two days of our simulations, the primary production difference turned to be limited again because the nGoM ecosystem shifted back to a nutrient-limited one.

In general, the influence of α_{sed} was significant as the underwater light for photosynthesis was limited by sediment-induced light attenuation and sediment concentration was moderately high. Although this study could not provide a widely accepted SSC range to determine whether α_{sed} played a vital role in photosynthesis and primary production, it confirmed that the ecosystem with greater variation of sediment concentration were surely affected by α_{sed}. The optical environment over the muddy inner Louisiana shelf, for example, was dominated by CDOM and chlorophyll under normal condition (D'Sa and Miller, 2003). During energetic events (e.g., hurricanes, cold fronts), however, high concentration of sediment particle due to strong resuspension became the most important light absorber. Given high frequency of cold fronts in winter and hurricanes in summer in the nGoM (Walker and Hammack, 2000; Keen et al., 2007), it was reasonable to speculate that coastal Louisiana ecosystem was potentially sensitive to α_{sed} not

https://doi.org/10.5194/bg-2020-58
Preprint. Discussion started: 25 March 2020

only on event scale, but also on annual and decadal scales. To confirm that, the long-term biogeochemical model studies focusing on the nGoM and Mississippi-Atchafalaya River system should explicitly include sediment-induced light attenuation in the future to better resolve photosynthesis and primary production.

4.5 Model uncertainties

The optical environment over the muddy Louisiana shelf is dominated by phytoplankton, suspended sediment, CDOM, and detritus particle (Le et al., 2014). So far, the model presented here only included the light attenuation due to the former two constituents, and the potential influence from CDOM and detritus warrants future study. Light attenuation due to detritus was simply parameterized using salinity in the previous model study (Justić and Wang, 2014), yet few biogeochemical models took light attenuation due to CDOM into account. In the nGoM, CDOM plays an indispensable role in modulating optical properties of inner shelf waters (D'Sa and Miller, 2003). To include CDOM-induced light attenuation into the biogeochemical models, a long-term CDOM climatology is required in future studies.

We used SeaWiFS-derived chlorophyll concentration to compare with our model results. However, deriving high quality chlorophyll data during hurricanes is still a challenge because: 1) thick clouds during hurricane limit the availability and quality of satellite images (Huang et al., 2011); 2) the uncertainty of chlorophyll estimation can be amplified due to strong CDOM absorption in the nGoM (D'Sa and Miller, 2003; D'Sa et al., 2006); and 3) conducting chlorophyll measurements during hurricane to calibrate bio-optical algorithms is still challenging. Given the rapid change and wide range of sediment and chlorophyll concentrations after hurricane, the algorithms based on observations under normal conditions might not be valid. To achieve high quality satellite-derived chlorophyll data for model validation, developing a new algorithm based on observations during hurricane events becomes essential.

In this study we simplified α_{sed} as a constant over the entire GoM following previous studies. When water is highly turbid, the availability of light for photosynthesis could be more related to sediment concentration rather than α_{sed} (McSweeney et al., 2017). Thus, using a constant to represent sediment light extinction coefficient when sediment concentration is high should not introduce considerable uncertainties. The optical characteristics of sediment particle, however, could greatly modify light availability underwater when SSC is relatively low (Storlazzi et al., 2015). Our sensitivity tests (section 4.4) also suggest the importance of α_{sed} in photosynthesis and primary production when resuspended sediment settled back on the sea floor. Therefore, it is necessary to apply an optimized α_{sed} parameterization to the regions where sediment dominates underwater optical environment.

Organic matter remineralization in sediments can dramatically increase nutrient concentration in the bottom boundary layer during strong resuspension (Couceiro et al., 2013). Field measurements after hurricanes Gustav and Ike suggested that the resuspension can expose the organic material in sediments to a more favorable environment for respiration (McCarthy et al., 2013). Nevertheless, so far most biogeochemical models neglect or simply parameterize this process (Fennel et al., 2006; Chai et al., 2007; Kishi et al., 2007). Moriarty et al. (2018) developed a particulate organic matter resuspension model and found remineralization intensity increased by an order of magnitude during moderate resuspension events in the nGoM. Given the strong storm-driven resuspension during hurricane, nutrient dynamics can be modified greatly by remineralization after the storm passage as well. An incorporation of organic matter resuspension

https://doi.org/10.5194/bg-2020-58
Preprint. Discussion started: 25 March 2020

Biogeosciences Discussions

and remineralization, together with the light attenuation effects addressed in this study, will complete our understanding of hurricane's impact on the biogeochemical cycling in shelf waters.

Our biogeochemical model only included freshwater and terrestrial nutrient input via river channel, while the importance of enhanced surface runoff and groundwater was not considered in our simulation. Du et al. (2019) estimated freshwater budget and found that surface runoff and groundwater accounted for ~34% of total freshwater load during hurricane Harvey. Although our understanding about nutrient flux associated with these two types of freshwater input is still limited, excluding surface runoff and groundwater flux in the model implies our underestimation of terrestrial nutrient discharge into the nGoM. Coupling groundwater and hydrology models with marine biogeochemical model in coastal regions is a feasible way to help us better understand the response of shelf ecosystem to terrestrial input.

5 Conclusions

We introduced a sediment-induced light attenuation algorithm to the coupled physical-biogeochemical model on the platform of ROMS. The new model reproduced the biogeochemical cycling during hurricane Gustav in the northern Gulf of Mexico. Improved model performance emphasized the importance of sediment in underwater optical environment and primary production during extreme weather events. During the passage of Gustav, the high SSC turned the inner shelf from a nutrient-limited environment to a light-limited one. NPP reduced from 1 to 0.2 g C/m^2/day. Due to the shading effect of resuspended sediment, the NPP recovered to pre-hurricane condition after one week of hurricane landing. As sediments further settled back on the seabed, nutrient accumulation and increased light availability incurred a strong surface post-hurricane bloom on the inner shelf. Nine days after Gustav's landing, the primary production below 20 m was still light-limited due to the unsettled sediments. The post-hurricane stratification, enhanced surface primary production, and other processes (e.g., respiration, remineralization) might intensify oxygen depletion and hypoxia formation in the shelf water. The post-hurricane bloom on the outer shelf was significantly enhanced by the laterally transported nutrients from the inner shelf. Suspended sediment affected primary production when SSC was moderately high after the landfall of Gustav. For those aquatic environments with great spatiotemporal variation of SSC (e.g., estuaries and lagoons), an optimal parameterization of sediment-induced light attenuation is imperative to better evaluate extreme weather events' impact on underwater productivity and biogeochemical cycling.

Acknowledgements
This study has been supported by NSF CyberSEES Award CCF-1856359, NASA (award number NNH17ZHA002C), Louisiana Board of Regents (award number NASA/LEQSF(2018-20)-Phase3-11), NSF Coastal SEES Award 1427389, and the LSU Foundation Billy and Ann Harrison Endowment for Sedimentary Geology. Computational support was provided by the High Performance Computing Facility (cluster Supermike II) at Louisiana State University. Model results used in this study are available at the LSU mass storage system and detailed information regarding the data set is posted on the homepage of Coupled Ocean Modeling Group (http://www.oceanography.lsu.edu/xuelab). Data request can be sent to the corresponding author via this webpage.

References

https://doi.org/10.5194/bg-2020-58
Preprint. Discussion started: 25 March 2020

Allison, M.A., Demas, C.R., Ebersole, B.A., Kleiss, B.A., Little, C.D., Meselhe, E.A., Powell, N.J., Pratt, T.C., Vosburg, B.M., 2012. A water and sediment budget for the lower Mississippi-Atchafalaya River in flood years 2008-2010: Implications for sediment discharge to the oceans and coastal restoration in Louisiana. J. Hydrol. 432–433, 84–97. https://doi.org/10.1016/j.jhydrol.2012.02.020

Arndt, S., Vanderborght, J., Regnier, P., 2007. Diatom growth response to physical forcing in a macrotidal estuary: Coupling hydrodynamics, sediment transport, and biogeochemistry. J. Geophys. Res. Ocean. 112.

Baker, E.T., Lavelle, J.W., 1984. Effect of Particle Size on the Light Attenuation Coefficient of Natural Suspensions. J. Geophys. Res. 89, 8197–8203. https://doi.org/10.1029/JC089iC05p08197

Bianucci, L., Balaguru, K., Smith, R.W., Leung, L.R., Moriarty, J.M., 2018. Contribution of hurricane-induced sediment resuspension to coastal oxygen dynamics. Sci. Rep. 8. https://doi.org/10.1038/s41598-018-33640-3

Bierman, V.J., Hinz, S.C., Zhu, D., Wiseman, W.J., Rabalais, N.N., Turner, R.E., 1994. A preliminary mass balance model of primary productivity and dissolved oxygen in the Mississippi River plume/inner Gulf Shelf region. Estuaries 17, 886–899.

Booij, N., Ris, R.C., Holthuijsen, L.H., 1999. A third-generation wave model for coastal regions: 1. Model description and validation. J. Geophys. Res. Ocean. 104, 7649–7666.

Chai, F., Jiang, M.S., Chao, Y., Dugdale, R.C., Chavez, F., Barber, R.T., 2007. Modeling responses of diatom productivity and biogenic silica export to iron enrichment in the equatorial Pacific Ocean. Global Biogeochem. Cycles 21, 1–16. https://doi.org/10.1029/2006GB002804

Cloern, J.E., 1987. Turbidity as a control on phytoplankton biomass and productivity in estuaries. Cont. Shelf Res. 7, 1367–1381.

Couceiro, F., Fones, G.R., Thompson, C.E.L., Statham, P.J., Sivyer, D.B., Parker, R., Kelly-Gerreyn, B.A., Amos, C.L., 2013. Impact of resuspension of cohesive sediments at the Oyster Grounds (North Sea) on nutrient exchange across the sediment-water interface. Biogeochemistry 113, 37–52. https://doi.org/10.1007/s10533-012-9710-7

D’Sa, E.J., Korobkin, M., Ko, D.S., 2011. Effects of Hurricane Ike on the Louisiana-Texas coast from satellite and model data. Remote Sens. Lett. 2, 11–19. https://doi.org/10.1080/01431161.2010.489057

D’Sa, E.J., Miller, R.L., 2003. Bio-optical properties in waters influenced by the Mississippi River during low flow conditions. Remote Sens. Environ. 84, 538–549. https://doi.org/10.1016/S0034-4257(02)00163-3

D’Sa, E.J., Miller, R.L., Del Castillo, C., 2006. Bio-optical properties and ocean color algorithms for coastal waters influenced by the Mississippi River during a cold front. Appl. Opt. 45, 7410–7428.

Davis, A., Yan, X.H., 2004. Hurricane forcing on chlorophyll-a concentration off the northeast coast of the U.S. Geophys. Res. Lett. 31, 4–7. https://doi.org/10.1029/2004GL020668

Devlin, M.J., Barry, J., Mills, D.K., Gowen, R.J., Foden, J., Sivyer, D., Tett, P., 2008. Relationships between suspended particulate material, light attenuation and Secchi depth in UK marine waters. Estuar. Coast. Shelf Sci. 79, 429–439. https://doi.org/10.1016/j.ecss.2008.04.024

https://doi.org/10.5194/bg-2020-58
Preprint. Discussion started: 25 March 2020

Biogeosciences Discussions
Open Access

Du, J., Park, K., Dellapenna, T.M., Clay, J.M., 2019. Dramatic hydrodynamic and sedimentary responses in Galveston Bay and adjacent inner shelf to Hurricane Harvey. Sci. Total Environ. 653, 554–564. https://doi.org/10.1016/j.scitotenv.2018.10.403

Fennel, K., Hetland, R., Feng, Y., Dimarco, S., 2011. A coupled physical-biological model of the Northern Gulf of Mexico shelf: Model description, validation and analysis of phytoplankton variability. Biogeosciences 8, 1881–1899. https://doi.org/10.5194/bg-8-1881-2011

Fennel, K., Wilkin, J., Levin, J., Moisan, J., O'Reilly, J., Haidvogel, D., 2006. Nitrogen cycling in the Middle Atlantic Bight: Results from a three-dimensional model and implications for the North Atlantic nitrogen budget. Global Biogeochem. Cycles 20, 1–14. https://doi.org/10.1029/2005GB002456

Fennel, K., Wilkin, J., Previdi, M., Najjar, R., 2008. Denitrification effects on air-sea CO2 flux in the coastal ocean: Simulations for the northwest North Atlantic. Geophys. Res. Lett. 35, 1–5. https://doi.org/10.1029/2008GL036147

Forbes, C., Luettich, R. a., Mattocks, C. a., Westerink, J.J., 2010. A Retrospective Evaluation of the Storm Surge Produced by Hurricane Gustav (2008): Forecast and Hindcast Results. Weather Forecast. 25, 1577–1602. https://doi.org/10.1175/2010WAF2222416.1

Ganju, N.K., Miselis, J.L., Aretxabaleta, A.L., 2014. Physical and biogeochemical controls on light attenuation in a eutrophic, back-barrier estuary. Biogeosciences 11, 7193–7205. https://doi.org/10.5194/bg-11-7193-2014

Gomez, F.A., Lee, S.K., Liu, Y., Hernandez, F.J., Muller-Karger, F.E., Lamkin, J.T., 2018. Seasonal patterns in phytoplankton biomass across the northern and deep Gulf of Mexico: A numerical model study. Biogeosciences 15, 3561–3576. https://doi.org/10.5194/bg-15-3561-2018

Haidvogel, D.B., Arango, H., Budgell, W.P., Cornuelle, B.D., Curchitser, E., Di Lorenzo, E., Fennel, K., Geyer, W.R., Hermann, A.J., Lanerolle, L., Levin, J., McWilliams, J.C., Miller, A.J., Moore, A.M., Powell, T.M., Shchepetkin, A.F., Sherwood, C.R., Signell, R.P., Warner, J.C., Wilkin, J., 2008. Ocean forecasting in terrain-following coordinates: Formulation and skill assessment of the Regional Ocean Modeling System. J. Comput. Phys. 227, 3595–3624. https://doi.org/10.1016/j.jcp.2007.06.016

Huang, W., Mukherjee, D., Chen, S., 2011. Assessment of Hurricane Ivan impact on chlorophyll-a in Pensacola Bay by MODIS 250m remote sensing. Mar. Pollut. Bull. 62, 490–498. https://doi.org/10.1016/j.marpolbul.2010.12.010

Hurst, N.R., White, J.R., Xu, K., Ren, M., 2019. Nitrate reduction rates in sediments experiencing turbulent flow conditions. Ecol. Eng. 128, 33–38. https://doi.org/10.1016/j.ecoleng.2018.12.027

Jacob, R., Larson, J., Everest, O., 2005. M x N Communication and Parallel Interpolation in Community Climate System Model Version 3 Using the Model Coupling Toolkit. Int. J. High Perform. Comput. Appl. 19, 293–307. https://doi.org/10.1177/1094342005056116

Justić, D., Wang, L., 2014. Assessing temporal and spatial variability of hypoxia over the inner Louisiana-upper Texas shelf: Application of an unstructured-grid three-dimensional coupled hydrodynamic-water quality model. Cont. Shelf Res. 72, 163–179. https://doi.org/10.1016/j.csr.2013.08.006

Keim, B.D., Muller, R.A., Stone, G.W., 2007. Spatiotemporal patterns and return periods of tropical storm and hurricane strikes from Texas to Maine. J. Clim. 20, 3498–3509. https://doi.org/10.1175/JCLI4187.1

Kishi, M.J., Kashiwai, M., Ware, D.M., Megrey, B.A., Eslinger, D.L., Werner, F.E., Noguchi-Aita, M., Azumaya, T., Fujii, M., Hashimoto, S., 2007. NEMURO—a lower trophic level model for the North Pacific marine ecosystem. Ecol. Modell. 202, 12–25.
Korobkin, M., D'Sa, E., Ko, D.S., 2009. Satellite observations and NCOM assessment of the Mississippi-Louisiana-Texas coast following hurricanes Gustav and Ike. Ocean. 2009 1–4. https://doi.org/10.23919/OCEANS.2009.5422213
Laurent, A., Fennel, K., Hu, J., Hetland, R., 2012. Simulating the effects of phosphorus limitation in the Mississippi and Atchafalaya river plumes. Biogeosciences 9, 4707–4723. https://doi.org/10.5194/bg-9-4707-2012
Le, C., Lehrter, J.C., Hu, C., Murrell, M.C., Qi, L., 2014. Spatiotemporal chlorophyll-a dynamics on the Louisiana continental shelf derived from a dual satellite imagery algorithm. J. Geophys. Res. Ocean. 119, 7449–7462.
Lin, S., Zou, T., Gao, H., Guo, X., 2009. The vertical attenuation of irradiance as a function of turbidity: a case of the Huanghai (Yellow) Sea in spring. Acta Oceanol. Sin. 28, 66–75.
Liu, K., Chen, Q., Hu, K., Xu, K., Twilley, R.R., 2018. Modeling hurricane-induced wetland-bay and bay-shelf sediment fluxes. Coast. Eng. 135, 77–90. https://doi.org/10.1016/j.coastaleng.2017.12.014
McCarthy, M.J., Carini, S.A., Liu, Z., Ostrom, N.E., Gardner, W.S., 2013. Oxygen consumption in the water column and sediments of the northern Gulf of Mexico hypoxic zone. Estuar. Coast. Shelf Sci. 123, 46–53. https://doi.org/10.1016/j.ecss.2013.02.019
McSweeney, J.M., Chant, R.J., Wilkin, J.L., Sommerfield, C.K., 2017. Suspended-Sediment Impacts on Light-Limited Productivity in the Delaware Estuary. Estuaries and Coasts 40, 977–993. https://doi.org/10.1007/s12237-016-0200-3
Meade, R.H., Moody, J.A., 2010. Causes for the decline of suspended-sediment discharge in the Mississippi River system, 1940-2007. Hydrol. Process. 24, 35–49.
Miller, W.D., Harding, L.W., Adolf, J.E., 2006. Hurricane Isabel generated an unusual fall bloom in Chesapeake Bay. Geophys. Res. Lett. 33, 2–5. https://doi.org/10.1029/2005GL025658
Moriarty, J.M., Harris, C.K., Fennel, K., Friedrichs, M.A.M., Xu, K., Rabouille, C., 2017. The roles of resuspension, diffusion and biogeochemical processes on oxygen dynamics offshore of the Rhône River, France: A numerical modeling study. Biogeosciences 14, 1919–1946. https://doi.org/10.5194/bg-14-1919-2017
Moriarty, J.M., Harris, C.K., Friedrichs, M.A.M., Fennel, K., Xu, K., 2018. Impact of seabed resuspension on oxygen and nitrogen dynamics in the northern Gulf of Mexico: A numerical modeling study. J. Geophys. Res. Ocean. 1–27. https://doi.org/10.1029/2018JC013950
Pan, G., Chai, F., Tang, D.L., Wang, D., 2017. Marine phytoplankton biomass responses to typhoon events in the South China Sea based on physical-biogeochemical model. Ecol. Modell. 356, 38–47. https://doi.org/10.1016/j.ecolmodel.2017.04.013
Pennock, J.R., 1985. Chlorophyll distributions in the Delaware estuary: regulation by light-limitation. Estuar. Coast. Shelf Sci. 21, 711–725.
Rabalais, N.N., Turner, R.E., Wiseman, W.J., 2001. Hypoxia in the Gulf of Mexico. J. Environ. Qual. 30, 320–329.
Saha, S., Moorthi, S., Pan, H.L., Wu, X., Wang, J., Nadiga, S., Tripp, P., Kistler, R., Woollen, J., Behringer, D., 2010. NCEP climate forecast system reanalysis (CFSR) 6-hourly products,

January 1979 to December 2010. Res. Data Arch. Natl. Cent. Atmos. Res. Comput. Inf. Syst. Lab. Boulder, CO.

Saha, S., Moorthi, S., Wu, X., Wang, J., Nadiga, S., Tripp, P., Behringer, D., Hou, Y.T., Chuang, H., Iredell, M., 2011. NCEP climate forecast system version 2 (CFSv2) 6-hourly products. Res. Data Arch. Natl. Cent. Atmos. Res. Comput. Inf. Syst. Lab.

Schaeffer, B.A., Sinclair, G.A., Lehrter, J.C., Murrell, M.C., Kurtz, J.C., Gould, R.W., Yates, D.F., 2011. An analysis of diffuse light attenuation in the northern Gulf of Mexico hypoxic zone using the SeaWiFS satellite data record. Remote Sens. Environ. 115, 3748–3757. https://doi.org/10.1016/j.rse.2011.09.013

Shchepetkin, A.F., McWilliams, J.C., 2005. The regional oceanic modeling system (ROMS): A split-explicit, free-surface, topography-following-coordinate oceanic model. Ocean Model. 9, 347–404. https://doi.org/10.1016/j.ocemod.2004.08.002

Skamarock, W.C., Klemp, J.B., Dudhi, J., Gill, D.O., Barker, D.M., Duda, M.G., Huang, X.-Y., Wang, W., Powers, J.G., 2005. A Description of the Advanced Research WRF Version 3. Tech. Rep. 113. https://doi.org/10.5065/D6DZ069T

Storlazzi, C.D., Norris, B.K., Rosenberger, K.J., 2015. The influence of grain size, grain color, and suspended-sediment concentration on light attenuation: Why fine-grained terrestrial sediment is bad for coral reef ecosystems. Coral Reefs 34, 967–975. https://doi.org/10.1007/s00338-015-1268-0

Tweel, A.W., Turner, R.E., 2012. Landscape-Scale Analysis of Wetland Sediment Deposition from Four Tropical Cyclone Events. PLoS One 7. https://doi.org/10.1371/journal.pone.0050528

Van Duin, E.H.S., Blom, G., Los, F.J., Maffione, R., Zimmerman, R., Cerco, C.F., Dortch, M., Best, E.P.H., 2001. Modeling underwater light climate in relation to sedimentation, resuspension, water quality and autotrophic growth. Hydrobiologia 444, 25–42. https://doi.org/10.1023/A:1017512614680

Walker, N.D., Hammack, A.B., 2000. Impacts of winter storms on circulation and sediment transport: Atchafalaya-Vermilion Bay region, Louisiana, USA. J. Coast. Res. 16, 996–1010. https://doi.org/10.2307/4300118

Walker, N.D., Leben, R.R., Balasubramanian, S., 2005. Hurricane-forced upwelling and chlorophyll a enhancement within cold-core cyclones in the Gulf of Mexico. Geophys. Res. Lett. 32, 1–5. https://doi.org/10.1029/2005GL023716

Warner, J.C., Armstrong, B., He, R., Zambon, J.B., 2010. Development of a Coupled Ocean-Atmosphere-Wave-Sediment Transport (COAWST) Modeling System. Ocean Model. 35, 230–244. https://doi.org/10.1016/j.ocemod.2010.07.010

Warner, J.C., Sherwood, C.R., Signell, R.P., Harris, C.K., Arango, H.G., 2008. Development of a three-dimensional, regional, coupled wave, current, and sediment-transport model. Comput. Geosci. 34, 1284–1306. https://doi.org/10.1016/j.cageo.2008.02.012

Wilson, R.F., Fennel, K., Paul Mattern, J., 2013. Simulating sediment-water exchange of nutrients and oxygen: A comparative assessment of models against mesocosm observations. Cont. Shelf Res. 63, 69–84. https://doi.org/10.1016/j.csr.2013.05.003

Wiseman, W.J., Rabalais, N.N., Turner, R.E., Dinnel, S.P., MacNaughton, A., 1997. Seasonal and interannual variability within the Louisiana coastal current: stratification and hypoxia. J. Mar. Syst. 12, 237–248.

https://doi.org/10.5194/bg-2020-58
Preprint. Discussion started: 25 March 2020

Xu, K., Harris, C.K., Hetland, R.D., Kaihatu, J.M., 2011. Dispersal of Mississippi and Atchafalaya sediment on the Texas-Louisiana shelf: Model estimates for the year 1993. Cont. Shelf Res. 31, 1558–1575. https://doi.org/10.1016/j.csr.2011.05.008

Xu, K., Mickey, R.C., Chen, Q., Harris, C.K., Hetland, R.D., Hu, K., Wang, J., 2016. Shelf sediment transport during hurricanes Katrina and Rita. Comput. Geosci. 90, 24–39. https://doi.org/10.1016/j.cageo.2015.10.009

Xue, Z., He, R., Fennel, K., Cai, W.J., Lohrenz, S., Hopkinson, C., 2013. Modeling ocean circulation and biogeochemical variability in the Gulf of Mexico. Biogeosciences 10, 7219–7234. https://doi.org/10.5194/bg-10-7219-2013

Yu, L., Fennel, K., Laurent, A., 2015. A modeling study of physical controls on hypoxia generationin the northern Gulf of Mexico. J. Geophys. Res. Ocean. 1–16. https://doi.org/10.1002/2014JC010472.

Zang, Z., Xue, Z.G., Bao, S., Chen, Q., Walker, N.D., Haag, A.S., Ge, Q., Yao, Z., 2018. Numerical study of sediment dynamics during hurricane Gustav. Ocean Model. 126, 29–42. https://doi.org/10.1016/j.ocemod.2018.04.002

Zang, Z., Xue, Z.G., Xu, K., Bentley, S.J., Chen, Q., D'Sa, E.J., Ge, Q., 2019. A Two Decadal (1993–2012) Numerical Assessment of Sediment Dynamics in the Northern Gulf of Mexico. Water 11, 938.

Zhu, Z., Ng, W., Liu, S., Zhang, J., Chen, J., Wu, Y., 2009. Estuarine phytoplankton dynamics and shift of limiting factors: A study in the Changjiang (Yangtze River) Estuary and adjacent area. Estuar. Coast. Shelf Sci. 84, 393–401.

https://doi.org/10.5194/bg-2020-58
Preprint. Discussion started: 25 March 2020

Biogeosciences Discussions
Open Access
EGU

Figure 1. panel a: Model domains applied in this study. The entire panel a is WRF model domain (6 km resolution) overlaid with water depth (color-shading). The black solid box represents model grid used by ROMS and SWAN with 5 km resolution. The black dashed line box (lat: 27°N–31°N; lon: 94°W–86°W) covers the northern Gulf of Mexico (nGoM). More details in the nGoM are shown in panel b. The thick purple/red lines indicate locations of 50m-isobath transect and transect D (Rabalais et al., 2001), respectively.

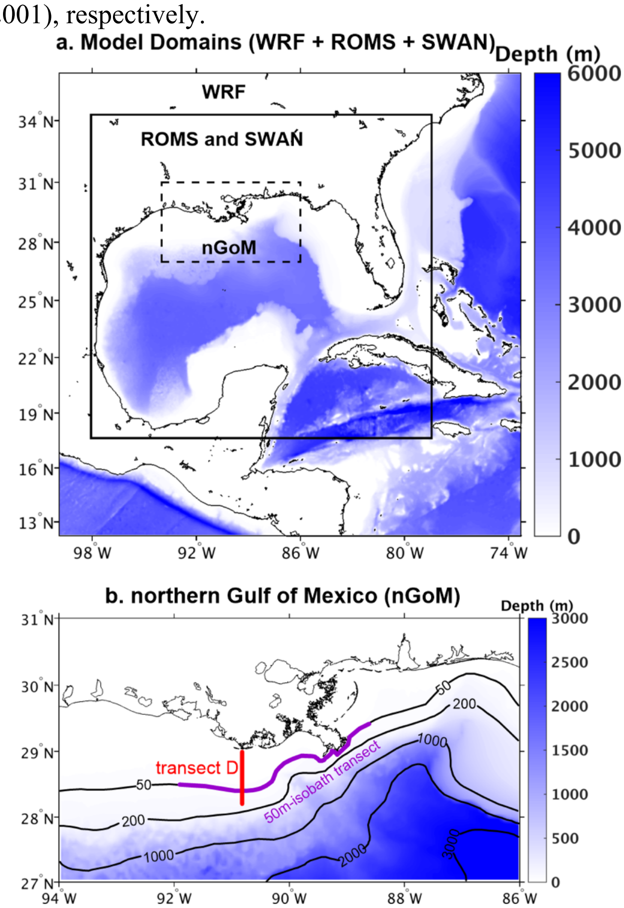

https://doi.org/10.5194/bg-2020-58
Preprint. Discussion started: 25 March 2020

Biogeosciences Discussions
Open Access
EGU

598 **Figure 2.** Flow chart of long-term (20 years) and hurricane (11 days) simulations. In step 1 we
599 only run ocean (ROMS) and biogeochemical (NEMURO) models, which provide initial inputs for
600 the next step. Step 2 couples ocean (ROMS), wave (SWAN), atmosphere (WRF), sediment
601 (CSTMS) and new biogeochemical (NEMURO) models with new sediment-induced light
602 attenuation term.

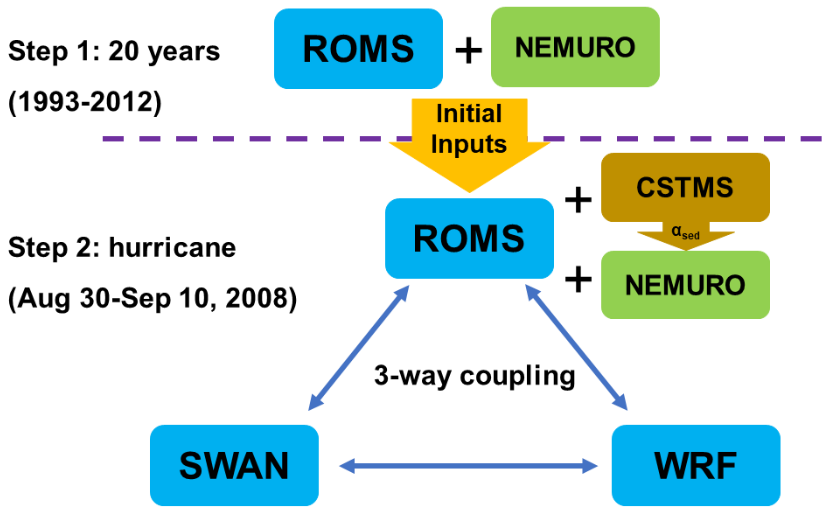

603
604

https://doi.org/10.5194/bg-2020-58
Preprint. Discussion started: 25 March 2020

Figure 3. Five-day composite of surface chlorophyll concentration in the year 2008: (a) SeaWiFS data before Gustav (August 25th–29th); (b) SeaWiFS data after Gustav (September 05th–09th); (c) benchmark run result ($\alpha_{sed} = 0.059$) after Gustav; (d) test 1 result ($\alpha_{sed} = 0$) after Gustav. White color in panels (a) and (b) represents no data available. Magenta curve shows hurricane track in panels b, c, and d. (BD: bird-foot delta; AS: Atchafalaya shelf).

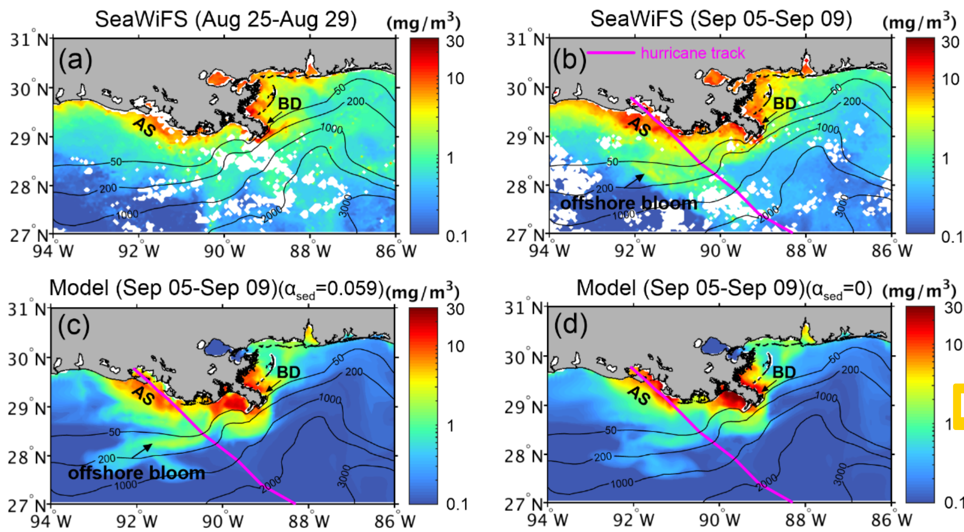

https://doi.org/10.5194/bg-2020-58
Preprint. Discussion started: 25 March 2020

Figure 4. Simulated five-day composite (September 05th–09th) of surface chlorophyll concentration after hurricane Gustav in comparison with corresponding SeaWiFS-derived surface chlorophyll results over the northern Gulf of Mexico inner shelf (h < 50 m). Model results is based on the benchmark run ($\alpha_{sed} = 0.059$) in panel a and test 1 ($\alpha_{sed} = 0$) in panel b.

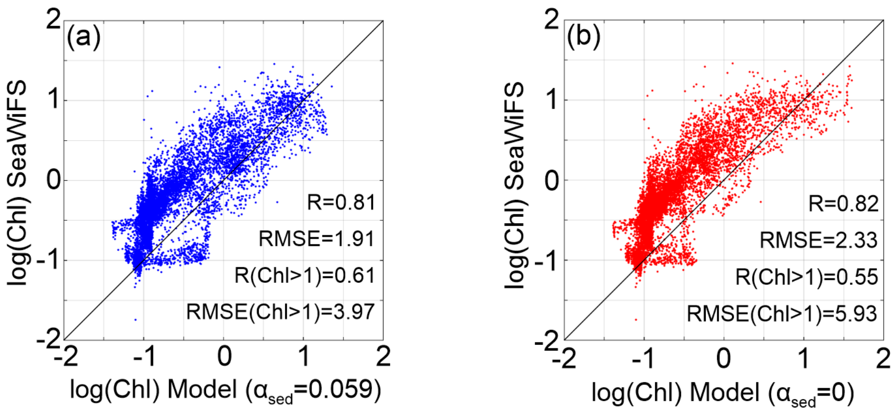

https://doi.org/10.5194/bg-2020-58
Preprint. Discussion started: 25 March 2020

Figure 5. Time series of spatial averaged (inner shelf) net primary production (a), surface chlorophyll concentration (b), NO_3 concentration (c), suspended sediment concentration (d), shortwave radiation (e), and sea surface temperature (f). In panels a, b, and c, blue represents benchmark run (α_{sed} = 0.059) and red represents test 1 (α_{sed} = 0). Dots in panel a are daily-averaged net primary production. The black dashed line shows Gustav landfall time.

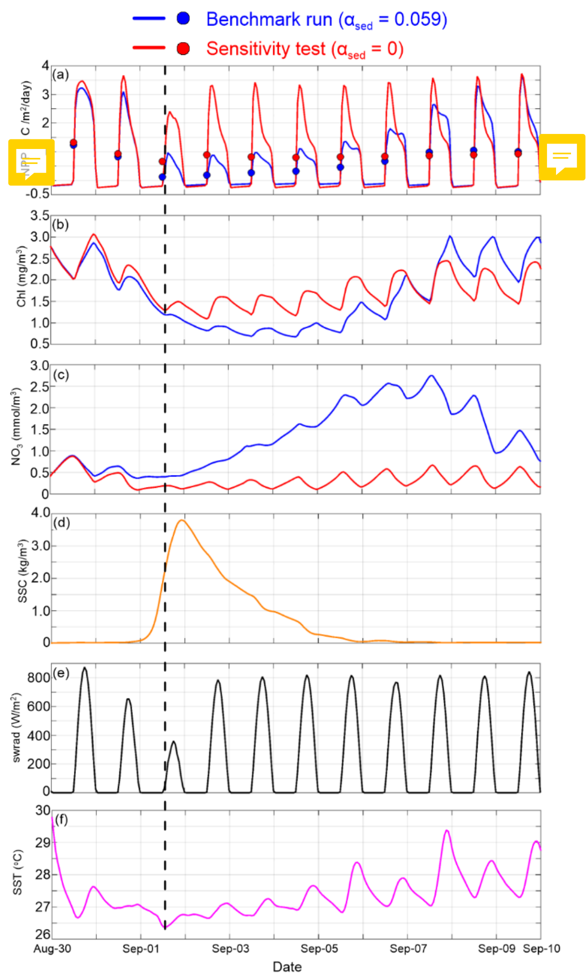

https://doi.org/10.5194/bg-2020-58
Preprint. Discussion started: 25 March 2020

Figure 6. Model simulated chlorophyll and suspended sediment concentration along transect D on August 31st (first row), September 2nd (second row), and September 10th (third row). The first and second columns represent chlorophyll concentrations of the test 1 and benchmark run, respectively (note the color scale is different from Fig. 1). The third column shows suspended sediment concentration.

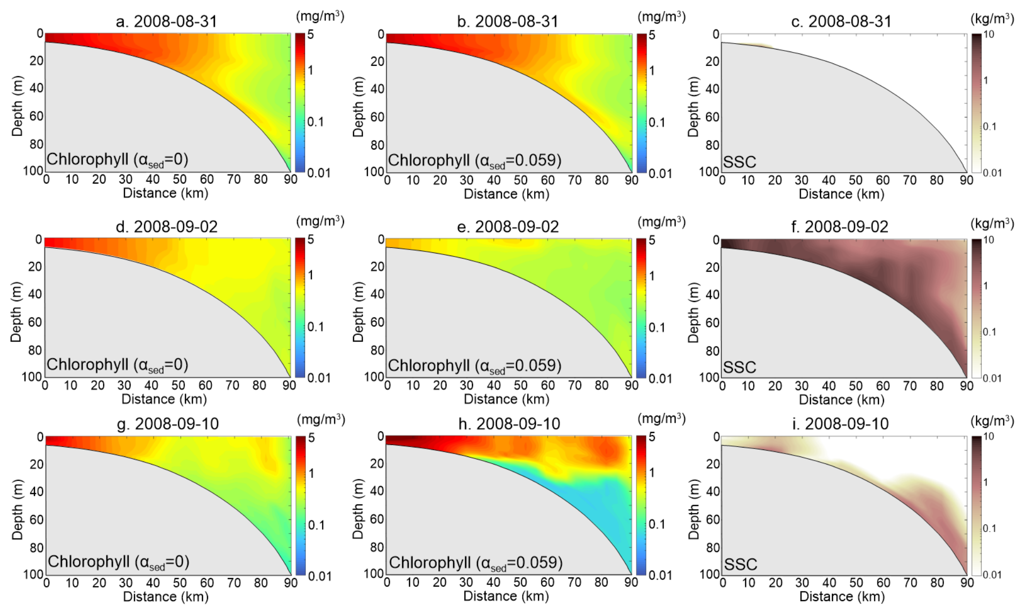

https://doi.org/10.5194/bg-2020-58
Preprint. Discussion started: 25 March 2020

Biogeosciences Discussions
Open Access

Figure 7. Comparison of spatial averaged (inner shelf) net primary production (panel a) and NO_3 concentration (panel b) between benchmark run (blue) and sensitivity tests with different α_{sed} (test 2: orange; test 3: cyan). The black dashed line shows Gustav landfall time.

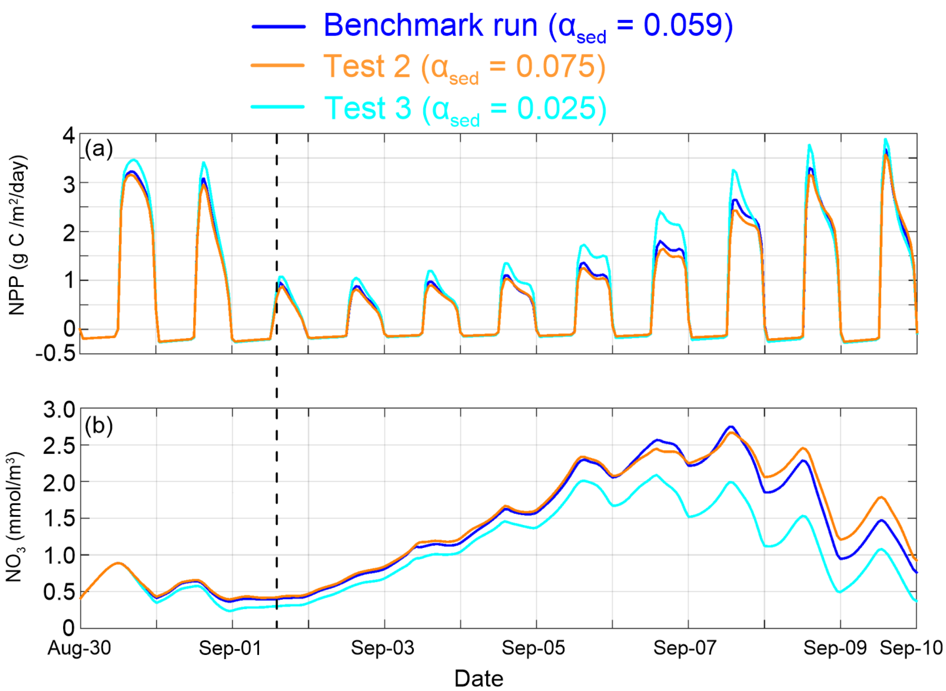

https://doi.org/10.5194/bg-2020-58
Preprint. Discussion started: 25 March 2020

Table 1. Offshore fluxes of NO_3 and chlorophyll along 50 m isobath transect (location see Fig. 1b).

	Net offshore NO_3 flux (mmol N/m/s)	Net offshore Chl flux (mg/m/s)
benchmark run ($\alpha_{sed} = 0.059$)	38.71	43.10
test 1 ($\alpha_{sed} = 0$)	7.35	66.88